Performance comparison between contrast source deterministic and probabilistic approaches

L. Poli, G. Oliveri, F. Viani, A. Massa

Abstract

In this report a comparison between the multi-task Bayesian Compressive Sensing based on the minimum-norm" (MN) current expansion and other contrast source inversion techniques of the state-of-the-art is proposed. More precisely, the conjugate gradient-based method and the non-linear procedure denoted as "non-radiating" approach have been considered for comparison.

1 Legend

- ST-BCS is the single-task Bayesian Compressive Sampling-based technique.
- MV-MT-BCS-Jmn is the multi-task Bayesian Compressive Sampling-based technique that exploits the correlation between the real and imaginary parts of the source, and between the views.
- CG is the contrast source conjugate gradient method.
- CG-NRS is the conjugate gradient method based on the non-radiating sources.

2 TEST CASE: Comparison with MV-MT-BCS-Jmn/CG/CG-NRS

Goal: show the performances of BCS with respect to other approaches at the state of the art

- Number of Views: V
- Number of Measurements: M
- Number of Cells for the Inversion: N
- Number of Cells for the Direct solver: D
- Side of the investigation domain: L

Test Case Description

Direct solver:

- Square domain divided in $\sqrt{D} \times \sqrt{D}$ cells
- Domain side: $L = 3\lambda$
- $D = 1296$ (discretization for the direct solver: $< \lambda/10$)

Investigation domain:

- Square domain divided in $\sqrt{N} \times \sqrt{N}$ cells
- $L = 3\lambda$
- $2ka = 2 \times \frac{2\pi}{\lambda} \times \frac{L\sqrt{2}}{2} = 6\pi\sqrt{2} = 26.65$
- $\#DOF = \frac{(2ka)^2}{2} = \frac{(2 \times \frac{2\pi}{\lambda} \times \frac{L\sqrt{2}}{2})^2}{2} = 4\pi^2 \left(\frac{L}{\lambda}\right)^2 = 4\pi^2 \times 9 \approx 355.3$
- N scelto in modo da essere vicino a $\#DOF$: $N = 324$ (18×18)

Measurement domain:

- Measurement points taken on a circle of radius $\rho = 3\lambda$
- Full-aspect measurements
- $M \approx 2ka \rightarrow M = 27$

Sources:

- Plane waves
- $V \approx 2ka \rightarrow V = 27$
- Amplitude $A = 1$
- Frequency: 300 MHz ($\lambda = 1$)

Object:

- Three Square Cylinders $L = 0.33\lambda$
- $\varepsilon_r \in \{1.5, 2.0, 2.5, 3.0\}$
- $\sigma = 0$ [S/m]

MV-MT-BCS-Jmn parameters:

- Gamma prior on noise variance parameter: $a = 5 \times 10^{0}$
- Gamma prior on noise variance parameter: $b = 2 \times 10^{-2}$
- Convergenze parameter: $\tau = 1.0 \times 10^{-8}$

CG parameters:

- Maximum number of Iterations: $I = 2000$
- Convergence: $\rho = 1 \times 10^{-5}$

CG-NRS (Non-Radiating Sources) parameters:

- Maximum number of Iterations: $I = 2000$
- Convergence: $\rho = 1 \times 10^{-5}$

RESULTS: Comparison with CG/CG-NCS - Three Square Cylinders $L = 0.33\lambda$ - $\varepsilon_r = 1.5$

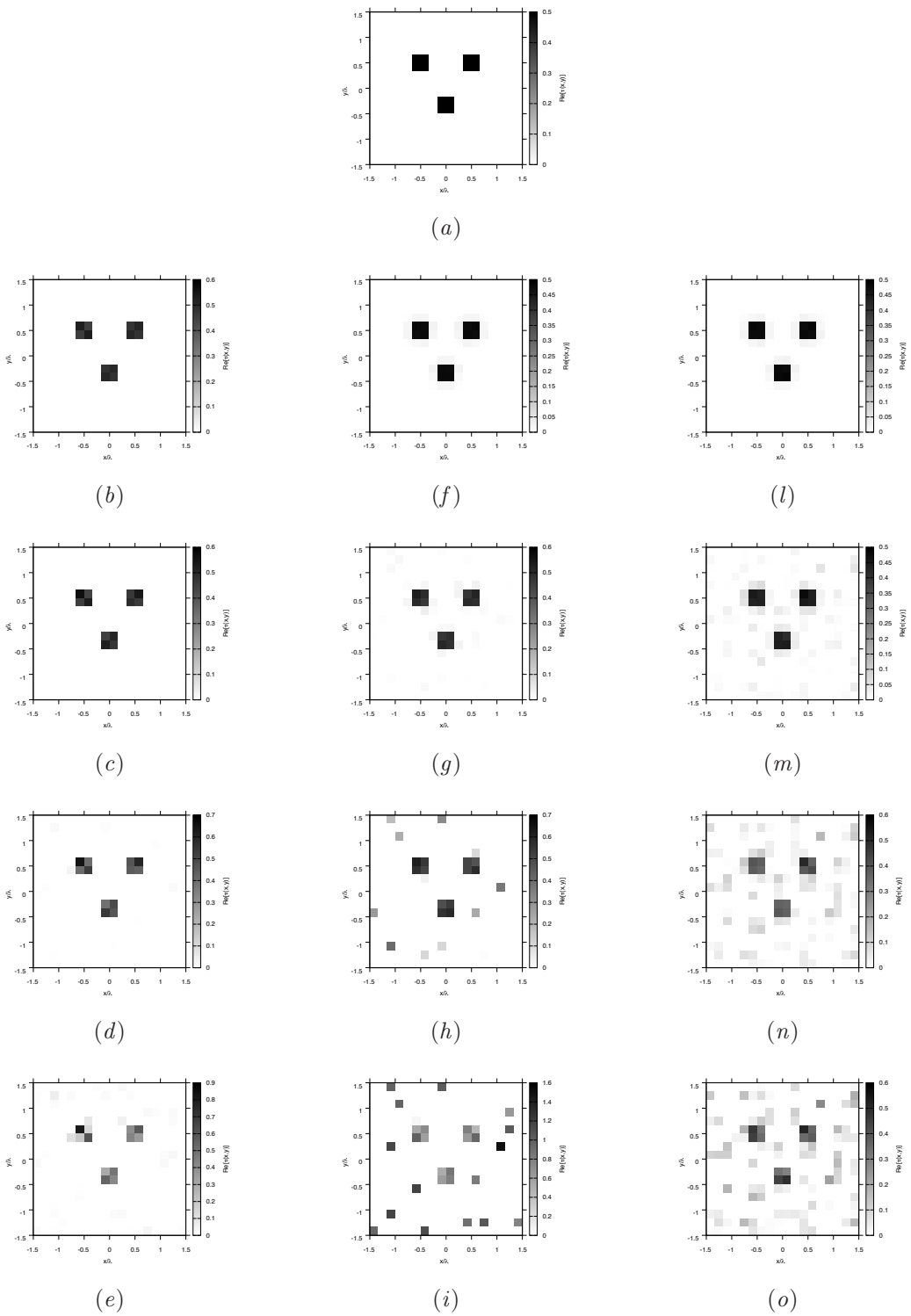

Figure 134. Actual object (a), (b)-(e) MV-MT-BCS-Jmn reconstructed (f)-(i) CG reconstructed, and (l)-(o) CG-NRS reconstructed object for $(b)(f)(l)$ $Noiseless$, $(c)(g)(m)$ $SNR = 20$ [dB] , $(d)(h)(n)$ $SNR = 10$ [dB] , $(e)(i)(o)$ $SNR = 5$ [dB].

RESULTS: Comparison with CG/CG-NCS - Three Square Cylinders $L = 0.33\lambda$ - $\varepsilon_r = 2.0$

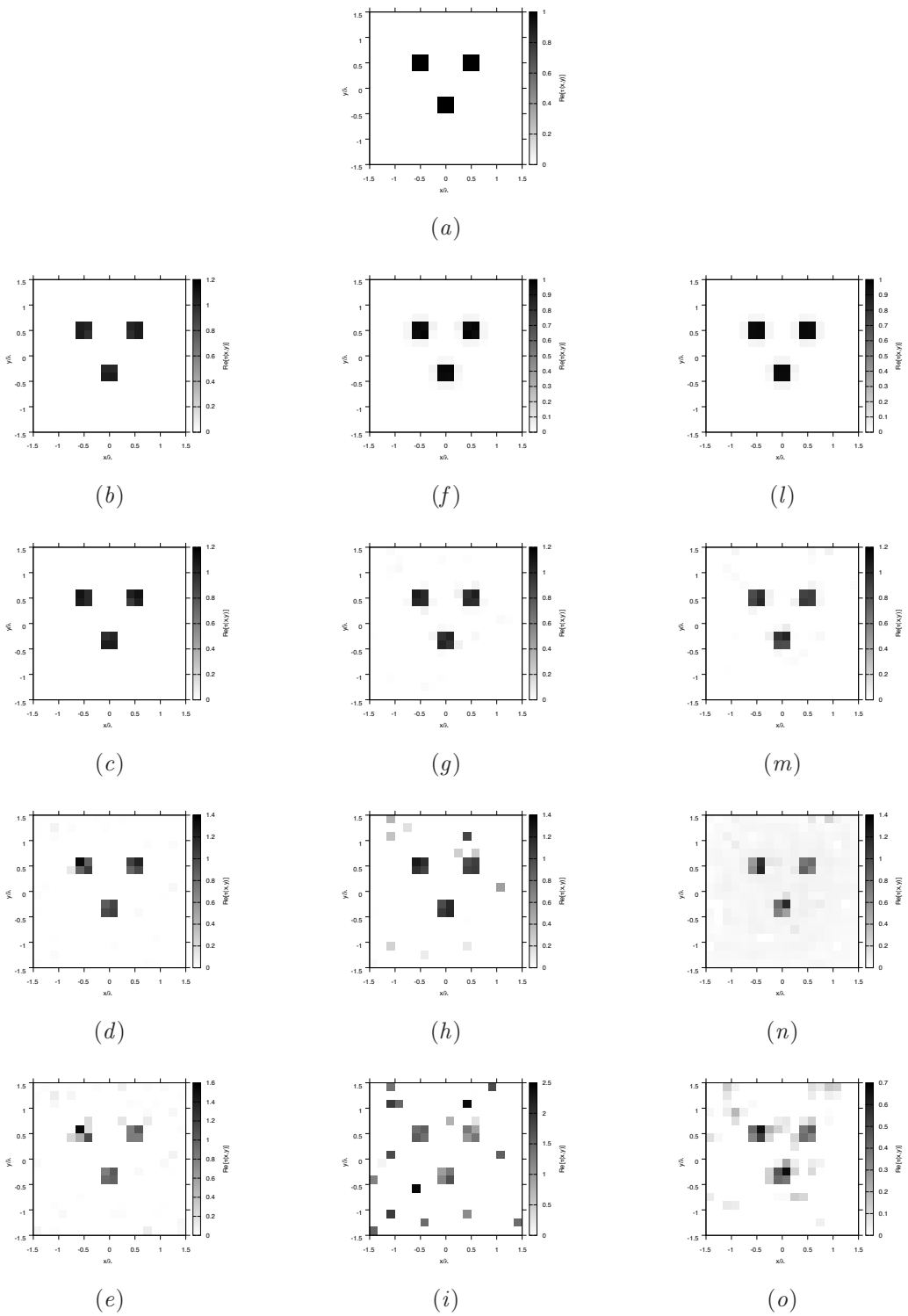

Figure 135. Actual object (a), (b)-(e) MV-MT-BCS-Jmn reconstructed (f)-(i) CG reconstructed, and (l)-(o) CG-NRS reconstructed object for $(b)(f)(l)$ $Noiseless$, $(c)(g)(m)$ $SNR = 20$ [dB] , $(d)(h)(n)$ $SNR = 10$ [dB] , $(e)(i)(o)$ $SNR = 5$ [dB].

RESULTS: Comparison with CG/CG-NCS - Three Square Cylinders $L = 0.33\lambda$ - $\varepsilon_r = 2.5$

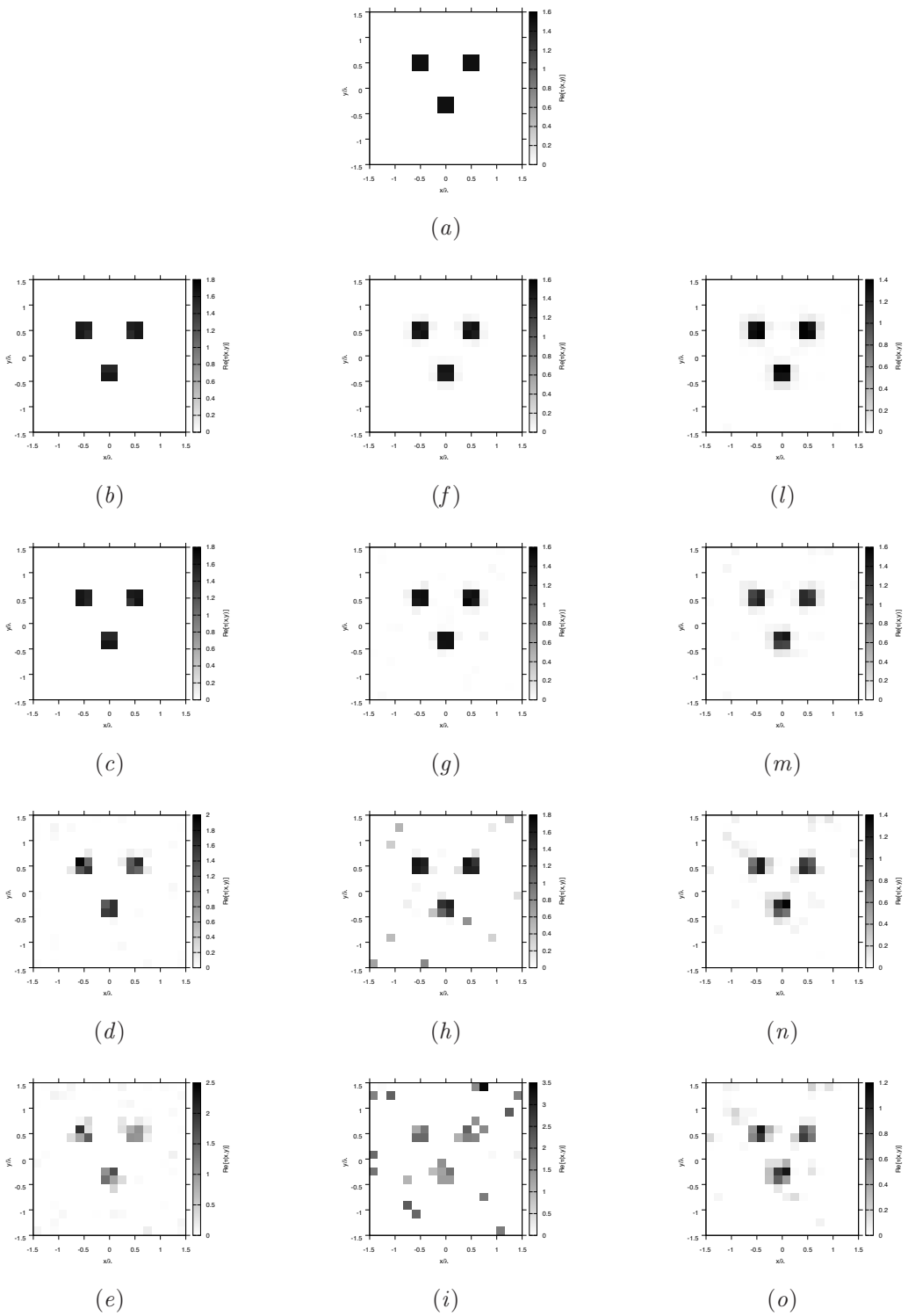

Figure 136. Actual object (a), (b)-(e) MV-MT-BCS-Jmn reconstructed (f)-(i) CG reconstructed, and (l)-(o) CG-NRS reconstructed object for $(b)(f)(l)$ $Noiseless$, $(c)(g)(m)$ $SNR = 20$ [dB] , $(d)(h)(n)$ $SNR = 10$ [dB] , $(e)(i)(o)$ $SNR = 5$ [dB].

RESULTS: Comparison with CG/CG-NCS - Three Square Cylinders $L = 0.33\lambda$ - $\varepsilon_r = 3.0$

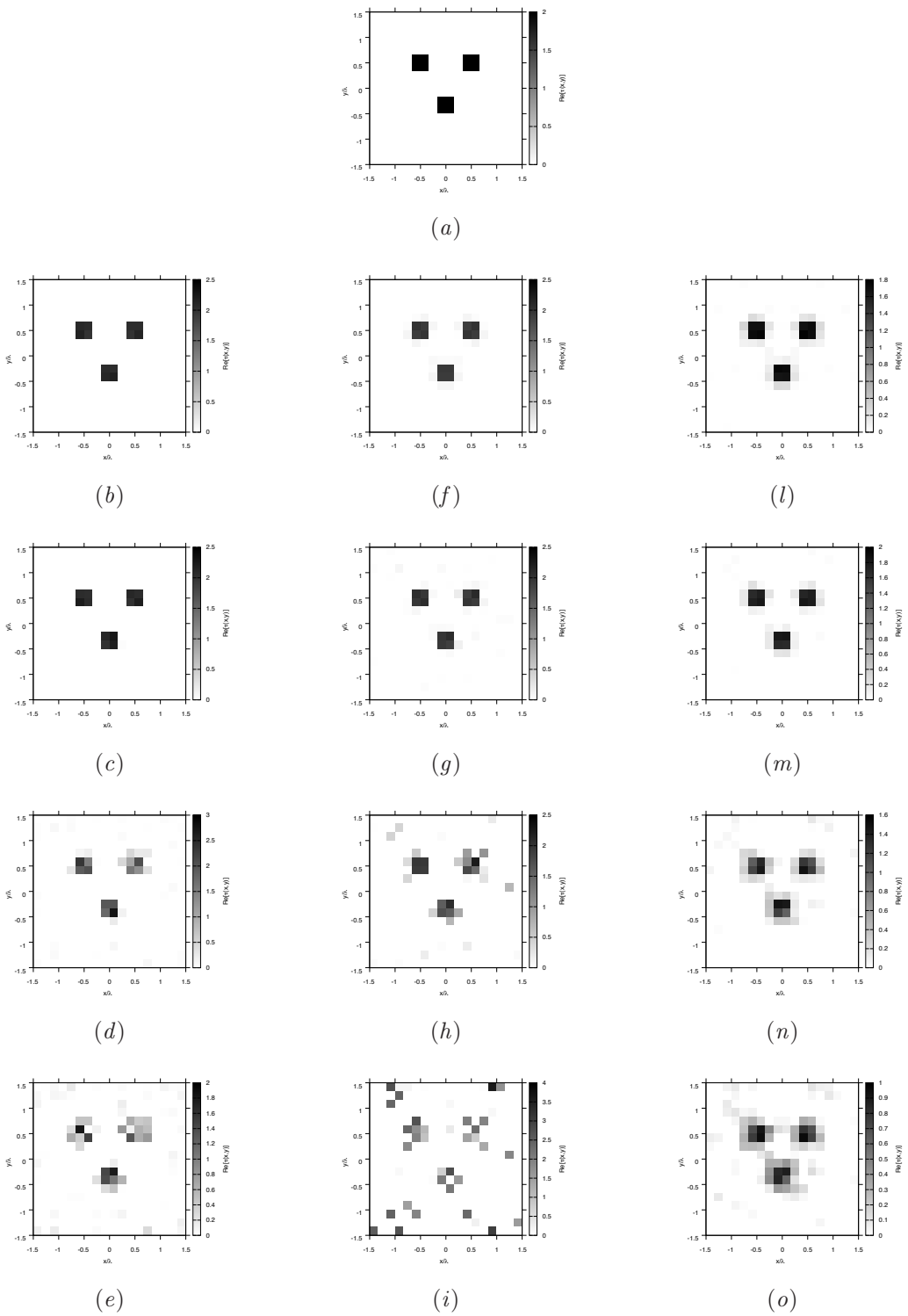

Figure 137. Actual object (a), (b)-(e) MV-MT-BCS-Jmn reconstructed (f)-(i) CG reconstructed, and (l)-(o) CG-NRS reconstructed object for $(b)(f)(l)$ $Noiseless$, $(c)(g)(m)$ $SNR = 20$ [dB] , $(d)(h)(n)$ $SNR = 10$ [dB] , $(e)(i)(o)$ $SNR = 5$ [dB].

RESULTS: Errors Comparison with CG/CG-NCS - $Noiseless$

ε_r	Technique	ξ_{tot}	ξ_{int}	ξ_{ext}
1.5	$MV-MT-BCS-Jmn$	5.59×10^{-4}	1.47×10^{-2}	0.00
	CG	1.92×10^{-3}	1.29×10^{-2}	1.49×10^{-3}
	$CG-NRS$	1.94×10^{-3}	1.19×10^{-2}	1.55×10^{-3}
2.0	$MV-MT-BCS-Jmn$	1.10×10^{-3}	2.31×10^{-2}	0.00
	CG	3.36×10^{-3}	1.54×10^{-2}	2.90×10^{-3}
	$CG-NRS$	3.77×10^{-3}	1.87×10^{-2}	3.08×10^{-3}
2.5	$MV-MT-BCS-Jmn$	1.58×10^{-3}	3.43×10^{-2}	0.00
	CG	4.66×10^{-3}	1.60×10^{-2}	4.23×10^{-3}
	$CG-NRS$	1.15×10^{-2}	6.17×10^{-2}	8.30×10^{-3}
3.0	$MV-MT-BCS-Jmn$	1.37×10^{-3}	2.97×10^{-2}	0.00
	CG	5.90×10^{-3}	1.77×10^{-2}	5.45×10^{-3}
	$CG-NRS$	2.00×10^{-2}	9.50×10^{-2}	1.54×10^{-2}

Table I. Comparison of error figures for MV-MT-BCS-Jmn, CG, and CG-NRS.

RESULTS: Errors Comparison with CG/CG-NCS - $SNR = 20dB$

ε_r	Technique	ξ_{tot}	ξ_{int}	ξ_{ext}
1.5	$MV-MT-BCS-Jmn$	9.24×10^{-4}	2.37×10^{-2}	0.00
	CG	1.79×10^{-3}	9.32×10^{-3}	1.50×10^{-3}
	$CG-NRS$	7.13×10^{-3}	3.89×10^{-2}	5.90×10^{-3}
2.0	$MV-MT-BCS-Jmn$	1.29×10^{-3}	2.85×10^{-2}	0.00
	CG	3.00×10^{-3}	1.39×10^{-2}	2.58×10^{-3}
	$CG-NRS$	6.14×10^{-3}	4.53×10^{-2}	3.31×10^{-3}
2.5	$MV-MT-BCS-Jmn$	1.71×10^{-3}	3.95×10^{-2}	0.00
	CG	4.68×10^{-3}	9.26×10^{-3}	4.50×10^{-3}
	$CG-NRS$	1.38×10^{-2}	8.19×10^{-2}	9.00×10^{-3}
3.0	$MV-MT-BCS-Jmn$	1.93×10^{-3}	4.04×10^{-2}	1.28×10^{-4}
	CG	5.93×10^{-3}	2.04×10^{-2}	5.37×10^{-3}
	$CG-NRS$	1.71×10^{-2}	8.17×10^{-2}	1.19×10^{-2}

Table II. Comparison of error figures for MV-MT-BCS-Jmn, CG, and CG-NRS.

RESULTS: Errors Comparison with CG/CG-NCS - $SNR = 10dB$

ε_r	Technique	ξ_{tot}	ξ_{int}	ξ_{ext}
1.5	$MV-MT-BCS-Jmn$	2.25×10^{-3}	4.60×10^{-2}	3.29×10^{-4}
	CG	8.54×10^{-3}	3.16×10^{-2}	7.65×10^{-3}
	$CG-NRS$	1.63×10^{-2}	7.33×10^{-2}	1.41×10^{-2}
2.0	$MV-MT-BCS-Jmn$	4.78×10^{-3}	5.51×10^{-2}	1.91×10^{-3}
	CG	1.29×10^{-2}	5.23×10^{-2}	1.13×10^{-2}
	$CG-NRS$	5.17×10^{-2}	1.34×10^{-1}	4.70×10^{-2}
2.5	$MV-MT-BCS-Jmn$	1.01×10^{-2}	8.03×10^{-2}	5.78×10^{-3}
	CG	2.11×10^{-2}	4.55×10^{-2}	2.02×10^{-2}
	$CG-NRS$	2.29×10^{-2}	1.83×10^{-1}	1.24×10^{-2}
3.0	$MV-MT-BCS-Jmn$	1.98×10^{-2}	1.16×10^{-1}	1.32×10^{-2}
	CG	3.03×10^{-2}	9.13×10^{-2}	2.79×10^{-2}
	$CG-NRS$	4.00×10^{-2}	2.46×10^{-1}	2.66×10^{-2}

Table III. Comparison of error figures for MV-MT-BCS-Jmn, CG, and CG-NRS.

RESULTS: Errors Comparison with CG/CG-NCS - $SNR = 5dB$

ε_r	Technique	ξ_{tot}	ξ_{int}	ξ_{ext}
1.5	$MV-MT-BCS-Jmn$	6.98×10^{-3}	1.01×10^{-1}	2.43×10^{-3}
	CG	5.27×10^{-2}	1.45×10^{-1}	4.92×10^{-2}
	$CG-NRS$	2.24×10^{-2}	7.05×10^{-2}	2.06×10^{-2}
2.0	$MV-MT-BCS-Jmn$	1.34×10^{-2}	1.19×10^{-1}	6.71×10^{-3}
	CG	8.23×10^{-2}	1.68×10^{-1}	7.89×10^{-2}
	$CG-NRS$	2.55×10^{-2}	2.74×10^{-1}	1.94×10^{-2}
2.5	$MV-MT-BCS-Jmn$	2.69×10^{-2}	1.96×10^{-1}	1.64×10^{-2}
	CG	1.07×10^{-1}	1.79×10^{-1}	1.05×10^{-1}
	$CG-NRS$	2.90×10^{-2}	2.91×10^{-1}	1.39×10^{-2}
3.0	$MV-MT-BCS-Jmn$	5.00×10^{-2}	3.30×10^{-1}	3.37×10^{-2}
	CG	1.66×10^{-1}	2.88×10^{-1}	1.61×10^{-1}
	$CG-NRS$	5.21×10^{-2}	3.96×10^{-1}	3.53×10^{-2}

Table IV. Comparison of error figures for MV-MT-BCS-Jmn, CG, and CG-NRS.

Observation:

$MV-MT-BCS-Jmn$ outperforms CG and $CG-NRS$ in terms of total ξ_{tot} error for every ε_r and SNR.

The internal error ξ_{int} is lower for CG wrt $MV-MT-BCS-Jmn$ and $CG-NRS$, except for the case $SNR = 5dB$.

References

[1] G. Oliveri, N. Anselmi, and A. Massa, "Compressive sensing imaging of non-sparse 2D scatterers by a total-variation approach within the Born approximation," IEEE Trans. Antennas Propag., vol. 62, no. 10, pp. 5157-5170, Oct. 2014.

[2] L. Poli, G. Oliveri, and A. Massa, "Imaging sparse metallic cylinders through a Local Shape Function Bayesian Compressive Sensing approach," Journal of Optical Society of America A, vol. 30, no. 6, pp. 1261-1272, 2013.

[3] F. Viani, L. Poli, G. Oliveri, F. Robol, and A. Massa, "Sparse scatterers imaging through approximated multitask compressive sensing strategies," Microwave Opt. Technol. Lett., vol. 55, no. 7, pp. 1553-1558, Jul. 2013.

[4] L. Poli, G. Oliveri, P. Rocca, and A. Massa, "Bayesian compressive sensing approaches for the reconstruction of two-dimensional sparse scatterers under TE illumination," IEEE Trans. Geosci. Remote Sensing, vol. 51, no. 5, pp. 2920-2936, May. 2013.

[5] L. Poli, G. Oliveri, and A. Massa, "Microwave imaging within the first-order Born approximation by means of the contrast-field Bayesian compressive sensing," IEEE Trans. Antennas Propag., vol. 60, no. 6, pp. 2865-2879, Jun. 2012.

[6] G. Oliveri, P. Rocca, and A. Massa, "A bayesian compressive sampling-based inversion for imaging sparse scatterers," IEEE Trans. Geosci. Remote Sensing, vol. 49, no. 10, pp. 3993-4006, Oct. 2011.

[7] G. Oliveri, L. Poli, P. Rocca, and A. Massa, "Bayesian compressive optical imaging within the Rytov approximation," Optics Letters, vol. 37, no. 10, pp. 1760-1762, 2012.

[8] L. Poli, G. Oliveri, F. Viani, and A. Massa, "MT-BCS-based microwave imaging approach through minimum-norm current expansion," IEEE Trans. Antennas Propag., vol. 61, no. 9, pp. 4722-4732, Sept. 2013.

[9] G. Oliveri, L. Lizzi, M. Pastorino, and A. Massa, "A nested multi-scaling inexact-Newton iterative approach for microwave imaging," IEEE Trans. Antennas Propag., vol. 60, no. 2, pp. 971-983, Feb. 2012.

[10] M. Salucci, D. Sartori, N. Anselmi, A. Randazzo, G. Oliveri, and A. Massa, "Imaging buried objects within the second-order Born approximation through a multiresolution-regularized inexact-Newton method", in 2013 International Symposium on Electromagnetic Theory (EMTS), (Hiroshima, Japan), pp. 116-118, May 20-24 2013T.

[11] P. Rocca, M. Carlin, L. Manica, and A. Massa, "Microwave imaging within the interval analysis framework," Progress in Electromagnetic Research, vol. 143, pp. 675-708, 2013.

[12] P. Rocca, M. Carlin, G. Oliveri, and A. Massa, "Interval analysis as applied to inverse scattering," IEEE International Symposium on Antennas Propag. (APS/URSI 2013), Chicago, Illinois, USA, Jul. 8-14, 2012.

[13] L. Manica, P. Rocca, M. Salucci, M. Carlin, and A. Massa, "Scattering data inversion through interval analysis under Rytov approximation," 7th European Conference on Antennas Propag. (EuCAP 2013), Gothenburg, Sweden, Apr. 8-12, 2013.

[14] P. Rocca, M. Carlin, and A. Massa, "Imaging weak scatterers by means of an innovative inverse scattering technique based on the interval analysis," 6th European Conference on Antennas Propag. (EuCAP 2012), Prague, Czech Republic, Mar. 26-30, 2012.